PCCP

Dynamic Article Links ▶

www.rsc.org/pccp

PAPER

Li self-diffusion in lithium niobate single crystals at low temperatures

J. Rahn,[a] **E. Hüger,**[a] **L. Dörrer,**[a] **B. Ruprecht,**[bc] **P. Heitjans**[bc] **and H. Schmidt***[ac]

Li self-diffusion in Li_2O-deficient $LiNbO_3$ single crystals is investigated in the temperature range between 423 and 773 K (150–500 °C) by secondary ion mass spectrometry. A thin layer of ion-beam sputtered isotope enriched $^6LiNbO_3$ was used as a tracer source, which allows one to study pure isotope interdiffusion. The diffusivities can be described by the Arrhenius law with an activation enthalpy of (1.33 ± 0.03) eV, which is in acceptable agreement with the migration energy of a single Li vacancy as determined by *ab initio* calculations given in the literature. Charge diffusivities as derived from impedance spectroscopy measurements on the same type of samples are identical to the tracer diffusivities within error limits. No indication of the formation of defect-complexes at low temperatures could be found in the diffusion behaviour.

1. Introduction

Lithium niobate ($LiNbO_3$) is one of the most technologically important oxides, with an extraordinary combination of ferroelectric, piezoelectric, acoustic, optical as well as ion conducting properties.[1–3] Large ferroelectric, pyroelectric and piezoelectric coefficients are present due to the polar asymmetry of the Li–O cage in the hexagonal crystal structure (space group $R3c$).[4–6] $LiNbO_3$ exhibits a wide solid solution region ranging from 44 mol% to about 50.5 mol% Li_2O.[7] Single crystals produced by the Czochralski method commonly show the congruent composition of about 48.5 mol% Li_2O. However, by using the vapor transport equilibration (VTE) method the synthesis of near stoichiometric crystals is also possible.[8] The change of composition from the lithium-poor compositions to the stoichiometric composition results in significant changes in the physical properties of the system, including the Curie temperature, the ferroelectric coercive field, and photorefractive properties.[1,9] These changes in physical properties are expected to be the result of defect clusters, which are also responsible for the non-stoichiometry. Several defect models are proposed,[2,8,10–14] while for the realization of the congruent composition the most reliable model consists of a niobium antisite atom which is compensated by four lithium vacancies ($Nb_{Li}^{\bullet\bullet\bullet\bullet} + 4V'_{Li}$).[13] In contrast, at and close to the stoichiometric composition Li Frenkel defects are expected.[13]

For many applications of lithium niobate, self-diffusion of the constituents is of high importance. Especially, the formation, stability and dissociation of defect clusters are closely related to diffusion properties. Further, it is of considerable interest[13] whether the defect clusters are expected to be long lived or whether the energy barriers to Li vacancy migration are sufficiently low so that the defect clusters might be highly dynamic, with Li vacancies diffusing among the various nearly energetically equivalent sites. If the defects are dynamic, the non-uniaxial components of the polarization of each individual cluster may dynamically cancel out locally.[13] Furthermore Li diffusivities are a measure for ionic transport properties and consequently for the ion conductivity.

While numerous studies on impurity diffusion are available for single crystalline $LiNbO_3$, reliable data on Li self-diffusion are very rare (for a review see ref. 13 and 15). Li is expected to be the most mobile species. Diffusion experiments are restricted to nuclear magnetic resonance (NMR) studies and also to impedance spectroscopy,[15–23] while most of the data are limited to the high temperature range above 773 K. There, diffusion is very fast and the defect complexes are destabilized. The only diffusion study based on mass tracers and stable isotopes was restricted to high temperatures above 1000 K.[15,24] Besides an ion conductivity study[16,21] no diffusivity data are available for single crystals below 773 K. An open question now is whether the diffusion mechanism at low and high temperatures is the same or whether it is changing due to the formation/dissociation of defect complexes or other processes.

In the present work, we investigated Li self-diffusion in L_2O-deficient $LiNbO_3$ single crystals in the temperature range between 423 and 773 K using secondary ion mass spectrometry. We used isotope enriched $^6LiNbO_3$ as a tracer reservoir. A sketch of the experimental arrangement is given in Fig. 1, where a thin isotope enriched layer of $^6LiNbO_3$ is deposited on the single crystal under investigation. The use of so-called isotope hetero-structures is an extremely reliable method to study self-diffusion processes in solids because pure isotope

[a] *Institut für Metallurgie, Thermochemie und Mikrokinetik, Technische Universität Clausthal, Clausthal-Zellerfeld, Germany. E-mail: harald.schmidt@tu-clausthal.de*
[b] *Institut für Physikalische Chemie und Elektrochemie, Leibniz Universität Hannover, Hannover, Germany*
[c] *ZFM—Zentrum für Festkörperchemie und Neue Materialien, Leibniz Universität Hannover, Hannover, Germany*
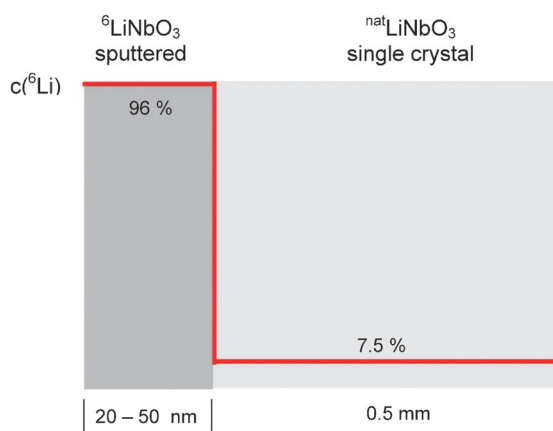
This journal is © the Owner Societies 2012

Phys. Chem. Chem. Phys., 2012, **14**, 2427–2433 | 2427

Fig. 1 Schematic representation of the diffusion experiment: 20–50 nm of LiNbO$_3$, composed of 96% ^{6}Li and 4% ^{7}Li (termed ^{6}LiNbO$_3$), is deposited *via* ion beam sputtering on a LiNbO$_3$ (0001) single crystal, composed of 7.5% ^{6}Li and 92.5% ^{7}Li isotopes (termed ^{nat}LiNbO$_3$).

interdiffusion takes place undisturbed from chemical gradients.[25–29] For comparison and in order to further elucidate details of the atomic transport properties, additional impedance spectroscopy measurements were done on the same type of single crystal.

2. Experimental details

The LiNbO$_3$ single crystals under investigation were supplied by Crystec (Berlin, Germany). The chemical composition was determined by UV absorption spectroscopy according to ref. 30 and 31. A Li$_2$O content of (48.5 ± 0.1) mol% was found which corresponds to the congruent composition of the phase diagram. 10 × 10 × 0.5 mm^3 *c*-axis oriented polished pieces were used for the experiments. Tracer deposition was carried out by depositing a 20–50 nm thin layer of isotope enriched ^{6}LiNbO$_3$ on the single crystal by ion beam sputtering, using a commercial set-up (IBC 681, Gatan) equipped with two Penning ion sources. Deposition was done at 5 keV and a current of about 200 μA in argon at an operating pressure of 5 × 10^{-3} mbar. The base vacuum was better than 5 × 10^{-7} mbar.

The sputter targets were prepared by solid state syntheses. Coarse Nb$_2$O$_5$ from Alfa Aesar (99.95%) was pestled to a fine powder in an agate mortar and mixed with enriched ^{6}Li$_2$CO$_3$ from Eurisotop (96% ^{6}Li). In order to account for loss of lithium in the sputtering process, the molar ratio of oxide and carbonate was chosen as 5 : 6. This results in targets of the composition 90% ^{6}LiNbO$_3$ + 10% ^{6}Li$_3$NbO$_4$. After subsequent ball milling of the powder mixture in a SPEX 8000M shaker mill, pellets of 2 cm in diameter were pressed and heated to 973 K with a rate of 2 K min^{-1}. The reaction step was followed by a sintering process at 1173 K for 12 h, which yielded polycrystalline dense targets. After tracer deposition, the sputtered layer consists of single phase LiNbO$_3$. This was proven by Grazing Incidence X-ray diffractometry on a 300 nm thin film which was annealed at 600 °C. Annealing induces crystallization and the formation of a polycrystalline film. No secondary phases (*e.g.* Li$_3$NbO$_4$ or LiNb$_3$O$_8$) were detected. Due to the fact that the tracer layer and single crystal have approximately the same chemical composition pure isotope interdiffusion is expected to be measured during the diffusion experiments.

For the diffusion experiments the coated samples were placed in a silica glass holder and introduced in the hot zone of a resistance furnace under ambient air conditions. The annealing time was between 30 min and 184 days at temperatures between 673 and 423 K. Additional diffusion annealing experiments were carried out in a commercial rapid thermal annealing setup (AO 500, MBE, Germany) in argon between 673 and 773 K. Here, extremely high heating rates are possible which allow one to realize annealing times down to several seconds.

The inward diffusion of the ^{6}Li from the sputter layer into the single crystal was determined by secondary ion mass spectrometry (SIMS) using a CAMECA IMS-3F machine. An O$^-$ primary ion beam (15 keV, 25 nA) was used in order to prevent electrical charging during the measurement. The sputtered area was about 250 μm × 250 μm. For further processing in a double focused mass spectrometer, the signal resulting from an area of about 110 μm × 110 μm in the centre was used in order to exclude effects resulting from the crater edge.

In the depth profiling mode, the secondary ion intensities of ^{6}Li$^+$ and ^{7}Li$^+$ ions were recorded as a function of sputter time. Since the two Li isotopes are chemically identical (neglecting the small isotope effect) for diffusion analysis the intensity of the signals is converted into ^{6}Li atomic fractions $c(x, t)$ according to

$$c(x, t) = \frac{I(^6\text{Li})}{I(^6\text{Li}) + I(^7\text{Li})} \quad (1)$$

Depth calibration was obtained by measuring the crater depth with a mechanical profilometer (Tencor, Alphastep).

For the impedance spectroscopy measurements single crystal slices with dimensions of 10 × 10 × 0.4 mm^3 were polished on both sides. Plane-parallel circular Ag electrodes of 5 mm in diameter were applied using silver conductive adhesive paste from Alfa Aesar. After drying the sample at 383 K additional Pt sheet contacts were glued on both sides with the same silver paste and fixed in a second drying step. Such electrodes withstand temperatures of 1000 K with no signs of damage.

AC impedance measurements in the frequency range from 5 Hz to 13 MHz with an alternating voltage of 0.125 V were carried out with a Hewlett Packard 4192A impedance analyzer and a home-built cell in air. A spring mechanism ensured that the sample was reliably connected to the jig. Temperature was measured using a type K thermocouple attached close to the sample and a Eurotherm temperature controlling unit.

3. Results

The ^{6}Li atomic fraction as a function of sputter depth is given in Fig. 2 for as-deposited samples annealed at 523 K for various times. With increasing annealing time the ^{6}Li tracer penetrates into the single crystal to depths of more than 200 nm. Experimentally determined depth profiles broadened after annealing can be described by the following solution of Fick's second law for self-diffusion across an interface[32]

$$c(x, t) = c_\infty + \frac{(c_0 - c_\infty)}{2}\left[\text{erf}\left(\frac{h + x}{R}\right) + \text{erf}\left(\frac{h - x}{R}\right)\right], \quad (2)$$
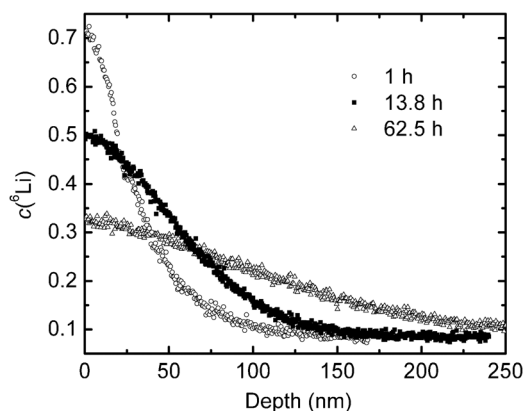
2428 | *Phys. Chem. Chem. Phys.*, 2012, **14**, 2427–2433

This journal is © the Owner Societies 2012

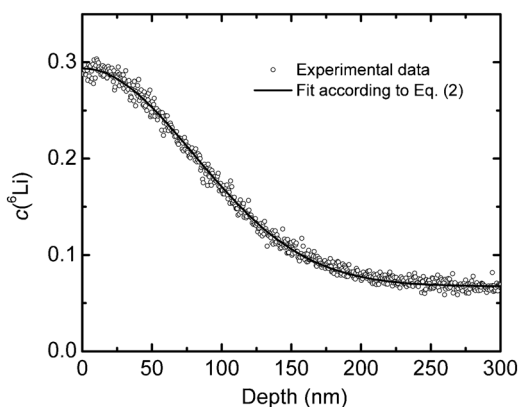**Fig. 2** Atomic fraction of ^{6}Li as a function of depth for a sample annealed at 523 K for 1, 13.8 and 62.5 h.

Fig. 3 Atomic fraction of ^{6}Li as a function of depth after annealing at 473 K for 34 days. A least-squares fit of eqn (2) to the experimental data is also indicated ($c_\infty = 0.075$, $c_0 = 0.96$, $h = 24$ nm, $R = 111$ nm).

where $c_\infty = 0.075$ is the natural abundance of ^{6}Li in the single crystal and $c_0 = 0.96$ that in the tracer layer. The original thickness of the as-deposited tracer layer is denoted as h, which was determined by SIMS to range between 20–50 nm, depending on the sample under investigation. The quantity R, describing the broadening of the tracer profile, is treated as a fit parameter. The self-diffusivity D at time t is determined from the difference in R of the diffusion profile and of the starting profile according to $D = (R^2(t) - R^2(0))/4t$. A typical example for an experimentally determined isotope depth profile and the corresponding fit is given in Fig. 3.

For the determination of diffusivities samples were used where the tracer significantly (at least 50 nm) penetrated into the single crystal (see Table 1). This was done in order to minimize possible fitting errors, which may result from low diffusion lengths. An overview on the results of the fitting procedures for all measurements is given in Table 1. It illustrates that no time dependence of diffusivities can be observed within error limits. An additional experiment was carried out, where a single crystal was pre-annealed at 1223 K (950 °C) for 12 h before tracer deposition and afterwards diffusion annealed for 61.4 h at 523 K (250 °C). The determined diffusivity of 2.2×10^{-20} m^2 s^{-1} is identical within error limits to the value given in Table 1.

Table 1 Compilation of the parameters of the diffusion experiment, where T is the annealing temperature, t is the annealing time, R is the diffusion length obtained from the fit, and D is the lithium diffusivity. Typical relative errors attributed to the diffusivities from the fitting of eqn (2) are about 30%

T/K	T/°C	t	R/nm	D/m^2 s^{-1}
423	150	35 d	33	3.8×10^{-23}
423	150	184 d	48	2.6×10^{-23}
448	175	593 h	55	2.9×10^{-22}
473	200	144 h	53	1.2×10^{-21}
473	200	816 h	111	1.0×10^{-21}
523	250	13.8 h	80	2.8×10^{-20}
523	250	62.5 h	129	1.8×10^{-20}
573	300	3 h	112	1.8×10^{-19}
623	350	0.5 h	112	1.7×10^{-18}
623	350	2.5 h	227	1.4×10^{-18}
673	400	5 min	171	2.4×10^{-17}
673	400	30 min	351	1.9×10^{-17}
723	450	75 s	178	1.0×10^{-16}
773	500	15 s	206	6.9×10^{-16}

In Fig. 4 the determined tracer diffusivities are plotted as a function of reciprocal temperature. For temperatures for which more than one diffusion anneal was carried out, the value with the largest broadening in R is displayed in Fig. 4. The data obey the Arrhenius law

$$D = D_0 \exp(-\Delta H/k_B T) \qquad (3)$$

A least-squares fit of eqn (3) to the diffusivities results in an activation enthalpy of $\Delta H = (1.33 \pm 0.03)$ eV and a pre-exponential factor of $D_0 = 1.7 \times 10^{-7}$ m^2 s^{-1} (error: ln D_0/m^2 s^{-1} = ±0.8) in the temperature range between 423 and 773 K. Note that the diffusivities vary over almost eight orders of magnitude.

Fig. 5(a) shows the ac conductivity as a function of frequency of a LiNbO$_3$ single crystal for temperatures between 776 K and 880 K. In the Cole-Cole plot of Fig. 5(b),
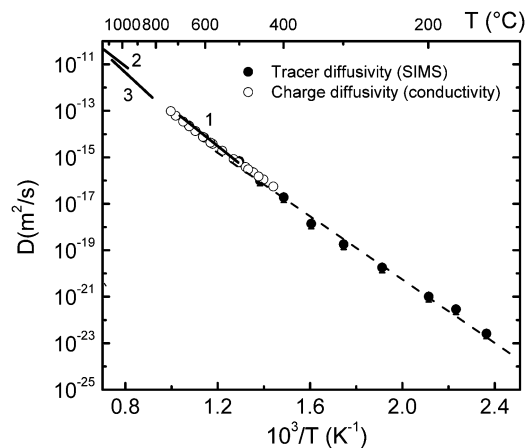

Fig. 4 Diffusivities of Li in a LiNbO$_3$ single crystal as a function of reciprocal temperature. Shown are tracer diffusivities measured by SIMS and charge diffusivities obtained by conductivity measurements. In the case of conductivity measurements, eqn (4) is used to calculate charge diffusivities. The dashed straight line corresponds to the Arrhenius fit of the SIMS data. For comparison, literature data taken from ref. 15 are given in the form of straight lines according to the following original references: (1) Halstead (NMR),[19] (2) Mehta et al. (ion conductivity)[20] and (3) Ptashnik et al. (tracer).[24]
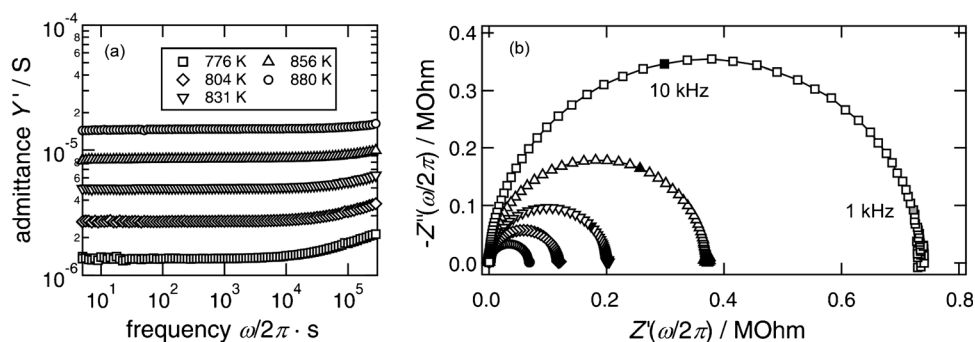
Fig. 5 (a) Real part of the admittance of a LiNbO$_3$ single crystal as a function of frequency for temperatures between 776 K and 880 K. (b) $-Z''(\omega)$ *vs.* $Z'(\omega)$ plot (Cole-Cole plot).

$-Z''(\omega)$ against $Z'(\omega)$, a single impedance arc is observed. A circle fit reveals a low inclination of less than 2 degrees for all temperatures. Accordingly, only low dispersion occurs in the admittance spectra $Y'(\omega)$ at high frequencies. An ideal Debye behavior which can be modeled by a single RC element with a single conductivity relaxation time $\tau = RC$ would result in perfect semicircles and a frequency independent value of $Y'(\omega)$, respectively. In contrast, for real ionic conductors dispersive, *i.e.* non-ideal, behavior has been identified as a "universal" property.[33] Intrinsically dispersive behavior can be ascribed to a distribution of relaxation times in the system.[34] From a microscopic point of view correlated forward–backward motion of the ions might also be responsible.[35–37] Models describing (conductivity) relaxation in real systems account for the effects being expected when structural disorder and Coulomb interactions are present in the system, which may also lead to a structural relaxation of the lattice.[38,39] Interesting microdynamic considerations more specifically for LiNbO$_3$, which might be useful for ongoing work, were already presented by Halstead in his early NMR paper.[19]

In our measurements the deviation from Debye relaxation is small which corresponds to the fact that effects of structural disorder or distributed jump barrier heights are in general not expected in a single crystal. Additionally, no distinct electrode effects appear at low frequencies showing that the application of Ag paste on the polished crystal surface yields low-resistance electrodes. The resistance $Z'(\omega)$ at the low-frequency intersection of the impedance arc in $Z(\omega)$ plots corresponds to the reciprocal DC plateau value of $Y'(\omega)$. Taking into account the sample dimensions, the dc conductivity σ can readily be calculated.

The conductivity measurements on a LiNbO$_3$ single crystal were carried out twice with different samples. Each sample was measured in several cycles with ascending and descending temperature values. For the sake of clarity only the data of one sample are depicted in Fig. 5 because both showed the same results. The data were recorded after a first heating to about 1000 K for several hours. DC conductivities were obtained which range from 2.8×10^8 S cm^{-1} at 694 K to $1.3 \cdot 10^5$ S cm^{-1} at 952 K.

For a comparison to the SIMS measurements charge diffusivities, D_σ, are calculated from the dc conductivities using the Nernst-Einstein relation,

$$D_\sigma = \frac{k_B T \sigma}{n q^2} \quad (4)$$

where n denotes the number density of the conducting species, $q = e$ the electrical charge, k_B the Boltzmann constant, and T the temperature. If it is assumed that all Li$^+$ ions are involved in the conduction process, $n = N/V$ is simply given by the number of Li$^+$ ions per unit cell $N = 6$ and the unit cell volume $V = 318$ Å^3. Since oxygen[40–42] and niobium[15] ion diffusivities are much lower than those of lithium, Li$^+$ is assumed to be the only effective charge carrier and the conductivity σ can therefore directly be used to calculate D_σ. The results are also plotted in Fig. 4 for comparison. It can be seen that the charge diffusivities are identical within error limits to the tracer diffusivities. Between 694 K and 952 K an Arrhenius behavior with an activation energy of $\Delta H_\sigma = (1.42 \pm 0.01)$ eV is found.

Generally, the ratio between tracer and charge diffusivity is given by the Haven ratio $H = D/D_\sigma$. In the actual case, a Haven ratio close to unity is found. This again confirms that Li is the only type of mobile species contributing to conductivity and that strong correlation effects are absent.

4. Discussion

In order to understand the Li diffusion behaviour in the LiNbO$_3$ single crystals under investigation, three enthalpies have to be considered, which might contribute to the activation enthalpy of diffusion, ΔH. These are the enthalpy of Li migration *via* a certain defect (vacancy or interstitial), ΔH_m, the enthalpy of formation of this defect, ΔH_f, and finally the enthalpy of defect complex formation at low temperatures, ΔH_c. Since the experimental data can be fitted with a unique Arrhenius straight line, only a single mechanism is dominant over the whole temperature range investigated. Due to the Li$_2$O deficient composition of the single crystal, intrinsic defect structures or defect clusters have to be present in order to realize off-stoichiometry. In the literature, there are mainly three models discussed for the intrinsic point defect structures in LiNbO$_3$.[13,14,20] In model I, two lithium vacancies are compensated by an oxygen vacancy ($2V'_{Li} + V_O^{\bullet\bullet}$), while in model II, niobium antisites are compensated by niobium vacancies ($5Nb_{Li}^{\bullet\bullet\bullet\bullet} + 4V_{Nb}^{'''''}$). The most reliable model (model III) consists of a niobium antisite compensated by four lithium vacancies ($Nb_{Li}^{\bullet\bullet\bullet\bullet} + 4V'_{Li}$). This model is supported by experimental X-ray and neutron diffraction studies[43,44] and density functional theory calculations.[45] As the dominant diffusion

defect the Li vacancy is assumed and *ab inito* DFT calculations for the migration enthalpy of single positively charged vacancies in LiNbO$_3$ give $\Delta H_m = 1.67$ eV.[13]

In ref. 46 the following solution reaction is given for Li$_2$O

$$\langle \text{LiNbO}_3 \rangle \leftrightarrow 3\,\text{Li}_2\text{O} + 4V'_{\text{Li}} + \text{Nb}^{\bullet\bullet\bullet\bullet}_{\text{Li}}, \qquad (5)$$
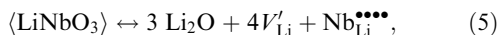
where $\Delta E = 4.56$ eV is the calculated energy of reaction (5) per Li$_2$O. Considering the equilibrium constant of reaction (5) of

$$K = a^3_{\text{Li}_2\text{O}} \times [V'_{\text{Li}}]^4 \times [\text{Nb}^{\bullet\bullet\bullet\bullet}_{\text{Li}}] = \exp\left(-\frac{\Delta G_r}{k_B T}\right) \qquad (6)$$

and the corresponding electro neutrality condition for Li$_2$O deficient single crystals

$$4[\text{Nb}^{\bullet\bullet\bullet\bullet}_{\text{Li}}] = [V'_{\text{Li}}] \qquad (7)$$

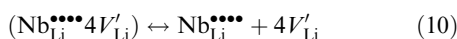we get for the concentration of lithium vacancies in equilibrium

$$[V'_{\text{Li}}] = a^{-3/5}_{\text{Li}_2\text{O}} \times 4^{1/5} \times \exp\left(-\frac{1}{5}\frac{\Delta G_r}{k_B T}\right). \qquad (8)$$

Here, ΔG_r is the standard Gibbs energy and $a_{\text{Li}_2\text{O}}$ is the activity of Li$_2$O. Assuming further a temperature independent activity of Li$_2$O and neglecting the enthalpy of dissolution of Li$_2$O in LiNbO$_3$,[41,42] we obtain for the formation enthalpy of Li vacancies,

$$\Delta H_f = -k_B \frac{\partial \ln[V'_{\text{Li}}]}{\partial(1/T)} = \frac{1}{5}\Delta H_r = 0.91 \text{ eV}. \qquad (9)$$

This vacancy formation enthalpy is assumed to play a considerable role at high temperatures where reaction (5) may take place and a modified defect equilibrium can be established by changing the temperature. In this case the sum of the contributions of defect formation and defect migration is expected for the activation enthalpy of diffusion, which is given by $\Delta H = \Delta H_m + \Delta H_f = 1.67$ eV + 0.91 eV = 2.58 eV. This value does not agree with the measured activation enthalpy of 1.33 eV.

In contrast, at low temperatures it is expected that defect clusters are formed, where the niobium antisite atom is surrounded by three lithium vacancies in nearest neighbour positions, plus one independent lithium vacancy along the z direction.[13,47] A possible dissociation of the defect complex can be written as

$$(\text{Nb}^{\bullet\bullet\bullet\bullet}_{\text{Li}}4V'_{\text{Li}}) \leftrightarrow \text{Nb}^{\bullet\bullet\bullet\bullet}_{\text{Li}} + 4V'_{\text{Li}} \qquad (10)$$

with the equilibrium constant

$$K^* = \frac{[\text{Nb}^{\bullet\bullet\bullet\bullet}_{\text{Li}}][V'_{\text{Li}}]^4}{[(\text{Nb}^{\bullet\bullet\bullet\bullet}_{\text{Li}}4V'_{\text{Li}})]} = K_0 \exp\left(-\frac{\Delta H_C}{kT}\right) \qquad (11)$$

At temperatures close to room temperature defect complexes in high concentration are expected to be present in order to explain the variation of physical properties within the solid solution range.[13] Increasing temperature leads to a shift of the equilibrium of eqn (10) to the right and free vacancies are formed which allow diffusion. An upper limit for the fraction of these vacancies is provided by the off-stoichiometry of the crystal, which is about 4% at the congruent composition.[14] At the medium range temperatures of our experiment this is the maximum amount of vacancies which can be used as transport

vehicles for diffusion. Lowering the temperature should lead to a decrease of the free vacancy concentration and consequently of the diffusivities by complex formation. At present the exact state and number of defect complexes at the temperatures of our measurements are not known. If defect complexes are present in a sufficient amount and if they are converted into Li vacancies, the activation enthalpy of Li diffusion should contain the sum of the enthalpy of the conversion reaction (10), as well as the enthalpy of motion of the vacancy. The formation enthalpy/energy of the defect complex discussed above, ΔH_c, was calculated by different authors to be 1.2 eV[13] and 0.77 eV,[48] respectively. We would get values of $\Delta H = \Delta H_m + \Delta H_c = 2.34$–2.87 eV, which is also inconsistent with the measured activation enthalpy. Consequently, the complexes are almost totally converted and the activation enthalpy of diffusion will be identical to the enthalpy of motion, $\Delta H = \Delta H_m$.

From our experiments an activation enthalpy of ionic motion of $\Delta H_m = 1.33$ eV is derived, which is in acceptable agreement to the value found by *ab initio* calculations.[13] Over the complete investigated temperature range Li vacancies are present and form the dominating defect governing diffusion. This is also valid at temperatures as low as 423 K. The fact that the migration enthalpy is measured in our experiments means that diffusion takes place at a constant vacancy concentration, even if the temperature is changed. This can be explained with a scenario that the dominating defect contribution is realized by reaction (5), however, it is not modified in the temperature range investigated. The single crystal was grown by the Czochralski method and the defect concentration was established during cooling. If temperature is progressively lowered, the rate constant in eqn (6) also becomes lower and the reaction "freezes in" at a certain temperature. This means that a constant vacancy concentration is present, which is not modified during the diffusion anneals, and we have some kind of "structural vacancies". As demonstrated by the pre-annealing experiment this "freezing-temperature" should be higher than 1223 K.

The pre-exponential factor in eqn (3) is than given by

$$D_0 = xa^2\nu_0\exp(\Delta S/k_B) \qquad (12)$$

where $a = 3.771$ Å[13] is the Li–Li jump distance, $x = [V'_{\text{Li}}]/\text{Li}^x_{\text{Li}} = 0.04$[14] is the mole fraction of Li vacancies and $\nu_0 \approx 2.5 \times 10^{13}$ s^{-1}[13] is a characteristic vibration frequency. If the entropy of ionic motion is assumed to be $\Delta S \approx 0$, the pre-exponential factor can be calculated according to eqn (12) to be $D_0 = 1.4 \times 10^{-7}$ m^2 s^{-1}. This is in excellent agreement with the experimentally derived value of 1.7×10^{-7} m^2 s^{-1} within error limits, confirming the suggested model.

In addition, the incorporation of a small amount of impurities in the form of aliovalent cations into the LiNbO$_3$ lattice may play a substantial role. Type and concentration of such impurities are unknown at present. As shown in ref. 48 various impurity incorporation reactions may lead to the extrinsic formation of Li vacancies. In this case also the migration enthalpy is measured in self-diffusion experiments. Diffusion experiments in single crystals, which were specifically doped, may give further clarification.

This journal is © the Owner Societies 2012

Phys. Chem. Chem. Phys., 2012, **14**, 2427–2433 | 2431

No significant influence of the formation of defect complexes on diffusion is observed. This can be explained by the fact that the formation of these complexes according to reaction (10) sets in for temperatures lower than 423 K. An alternative explanation might be that reaction (10) is not in equilibrium at the temperature under investigation. The corresponding rate constant that governs the establishment of the equilibrium and the formation of complexes might be very small in the temperature domain investigated. Hence, a significant time dependent decrease of the diffusivity might be expected for long annealing times, which, however, is not found up to now. Further insight into this topic might be possible if diffusion measurements will be carried out very close to room temperature, where defect complexes are present, as indicated by measurements of ferroelectric properties.[9] In order to clarify this open question, a different method of diffusivity determination has to be applied, which is able to determine diffusivities well below 10^{-23} m^2 s^{-1}. Neutron reflectometry might be such a method.[49]

Our measurements provided the first tracer self-diffusivities in LiNbO$_3$ single crystals at temperatures below 773 K. However, in the literature some high-temperature data above 1073 K are available, which were also obtained by tracer methods about 25 years ago.[24] The data are also shown in Fig. 4. A higher activation enthalpy of 1.98 eV was found. This can be explained by the fact that in this temperature range significant vacancy formation according to reaction (5) takes place. The activation enthalpy is then given by $\Delta H = \Delta H_m + \Delta H_f = 1.33$ eV $+ 0.92$ eV ≈ 2.2 eV, being close to the measured value. Further self-diffusivities in the high-temperature range are displayed in Fig. 4, which were obtained by NMR by Halstead[19] and also by conductivity measurements by Metha et al.[20] Halstead's data nicely correspond to our charge diffusivity data. The slightly higher activation enthalpies of diffusion of 1.55 eV and 1.46–1.62 eV found by Mehta et al. and Halstead, respectively, might be a hint that around these temperatures vacancy formation according to reaction (5) might start to influence the data. In order to correctly understand the diffusion behaviour it has to be kept in mind that the exact chemical composition of LiNbO$_3$ in its solid solution range is not known for the literature data. This also might contribute to differences in the activation enthalpy.

5. Conclusion

We employed tracer diffusivity measurements using SIMS depth profiling and impedance spectroscopy in order to obtain precise data for lithium self-diffusion in Li$_2$O-deficient LiNbO$_3$ single crystals at low temperatures. In the temperature range between 423 and 773 K (150–500 °C) diffusion of lithium is governed by a single vacancy mechanism with an activation enthalpy of diffusion of 1.33 eV. Lithium diffuses via structural vacancies whose concentration is fixed by a frozen-in defect structure formed during synthesis of the single crystal. Therefore, the measured activation enthalpy of diffusion essentially consists of the migration enthalpy of lithium vacancies. Charge diffusivities derived from conductivity measurements are in good accordance with the tracer diffusivities pointing to a Haven ratio close to one.

References

1 V. Gopalan, V. Dierolf and D. A. Scrymgeou, *Annu. Rev. Mater. Res.*, 2008, **37**, 449.
2 *Properties of Lithium Niobate*, ed. K. K. Wong, Inspec, London, 2002.
3 T. Volk and M. Wöhlecke, *Lithium Niobate*, Springer, Berlin, 2010.
4 S. C. Abrahams, J. M. Reddy and J. L. Bernstin, *J. Phys. Chem. Solids*, 1966, **27**, 997.
5 H. D. Megaw, *Acta Crystallogr., Sect. A: Cryst. Phys., Diffr., Theor. Gen. Crystallogr.*, 1968, **24**(6), 583.
6 R. S. Weis and T. K. Gaylord, *Appl. Phys. A: Mater. Sci. Process.*, 1985, **37**, 191.
7 P. Lerner, C. Legras and J. Dumas, *J. Cryst. Growth*, 1968, **3**, 231.
8 P. F. Bordui, R. G. Norwood, D. H. Jundt and M. M. Fejer, *J. Appl. Phys.*, 1992, **71**, 875.
9 V. Gopalan, T. E. Mitchell, Y. Furukawa and K. Kitamura, *Appl. Phys. Lett.*, 1998, **72**, 1981.
10 O. F. Schirmer, O. Thiemann and M. Wohlecke, *J. Phys. Chem. Solids*, 1991, **52**, 185.
11 A. Prokhorov and I. Kuzminov, *Physics and Chemistry of Crystalline Lithium Niobate*, Hilger, Bristol, 1990.
12 S. C. Abrahams and P. Marsh, *Acta Crystallogr., Sect. B: Struct. Sci.*, 1986, **42**, 61.
13 H. Xu, D. Lee, S. B. Sinnott, V. Dierolf, V. Gopalan and S. R. Phillpot, *J. Phys.: Condens. Matter*, 2010, **22**, 135002.
14 J. Shi, H. Fritze, G. Borchardt and K.-D. Becker, *Phys. Chem. Chem. Phys.*, 2011, **13**, 6925.
15 D. Birnie III, *J. Mater. Sci.*, 1993, **28**, 302.
16 P. Heitjans, M. Masoud, A. Feldhoff and M. Wilkening, *Faraday Discuss.*, 2007, **134**, 67.
17 M. Wilkening, D. Bork, S. Indris and P. Heitjans, *Phys. Chem. Chem. Phys.*, 2002, **4**, 3246.
18 M. Wilkening and P. Heitjans, *Solid State Ionics*, 2006, **177**, 3031.
19 T. K. Halstead, *J. Chem. Phys.*, 1970, **53**, 3427.
20 A. Mehta, E. K. Chang and D. M. Smyth, *J. Mater. Res.*, 1991, **6**, 851.
21 M. Masoud and P. Heitjans, *Def. Diff. Forum*, 2005, **237–240**, 1016.
22 D. Bork and P. Heitjans, *J. Phys. Chem. B*, 1998, **102**, 7303.
23 D. Bork and P. Heitjans, *J. Phys. Chem. B*, 2001, **105**, 9162.
24 V. B. Ptashnik, T. Y. Dunaeva and I. V. Myasnikov, *Inorg. Mater.*, 1985, **21**, 1814.
25 H. Schmidt, G. Borchardt, C. Schmalzried, R. Telle, S. Weber and H. Scherrer, *J. Appl. Phys.*, 2003, **93**, 907.
26 H. Schmidt, U. Geckle and M. Bruns, *Phys. Rev. B: Condens. Matter Mater. Phys.*, 2006, **74**, 045203.
27 E. Hüger, U. Tietze, D. Lott, H. Bracht, E. E. Haller, D. Bougeard and H. Schmidt, *Appl. Phys. Lett.*, 2008, **93**, 162104.
28 H. D. Fuchs, W. Walukiewicz, E. E. Haller, R. Schorer, G. Abstreiter, A. I. Rudnev, A. V. Tikhomirov and V. I. Ozhogin, *Phys. Rev. B: Condens. Matter Mater. Phys.*, 1995, **51**, 16817.
29 H. A. Bracht, H. H. Silvestri and E. E. Haller, *Solid State Commun.*, 2005, **133**, 727.
30 I. Földvari, K. Polgar, R. Voszka and R. N. Balasanyan, *Cryst. Res. Technol.*, 1984, **19**, 1659.
31 Y. Kong, W. Zhang, X. Chen, J. Xu and G. Zhang, *J. Phys.: Condens. Matter*, 1999, **11**, 2139.
32 J. Crank, *The Mathematics of Diffusion*, Oxford University Press, Oxford, 1975.
33 A. K. Jonscher, *Nature*, 1977, **267**, 673.
34 A. K. Jonscher, *J. Mater. Sci.*, 1978, **13**, 553.
35 P. Maass, J. Petersen, A. Bunde, W. Dieterich and H. E. Roman, *Phys. Rev. Lett.*, 1991, **66**, 52.
36 M. Meyer, P. Maass and A. Bunde, *Phys. Rev. Lett.*, 1993, **71**, 573.
37 K. Funke, *Solid State Ionics*, 1988, **28–30**, 100.

2432 | *Phys. Chem. Chem. Phys.*, 2012, **14**, 2427–2433

This journal is © the Owner Societies 2012

38 P. Maass, J. Petersen and A. Bunde, *Phys. Rev. B: Condens. Matter Mater. Phys.*, 1995, **51**, 8164.

39 K. Funke, *Prog. Solid State Chem.*, 1993, **22**, 111.

40 P. J. Jorgensen and R. W. Bartlett, *J. Phys. Chem. Solids*, 1969, **30**, 2639.

41 P. Fielitz, G. Borchardt, R. De Souza, M. Martin, M. Masoud and P. Heitjans, *Sol. State Sci.*, 2008, **10**, 746.

42 P. Fielitz, O. Schneider, G. Borchardt, A. Weidenfelder, H. Fritze, J. Shi, K. D. Becker, S. Ganschow and B. Bertram, *Solid State Ionics*, 2011, **189**, 1.

43 N. Zotov, H. Boysen, F. Frey, T. Metzger and E. Born, *J. Phys. Chem. Solids*, 1994, **55**, 145.

44 G. S. Zhdanov, S. A. Ivanov, W. V. Kolontsova and A. E. Korneev, *Ferroelectrics*, 1978, **21**, 463.

45 H. X. Xu, D. Lee, J. He, S. B. Sinnott, V. Gopalan, V. Dierolf and S. R. Phillpot, *Phys. Rev. B: Condens. Matter Mater. Phys.*, 2008, **78**, 174103.

46 H. J. Donnerberg, S. M. Tomlinson and C. R. A. Catlow, *J. Phys. Chem. Solids*, 1991, **52**, 201.

47 S. Kim, V. Gopalan, K. Kitamura and Y. Furukawa, *J. Appl. Phys.*, 2001, **90**, 2949.

48 R. M. Araujo, K. Lengyel, R. A. Jackson, L. Kovacs and M. E. G. Valerio, *J. Phys.: Condens. Matter*, 2007, **19**, 046211.

49 H. Schmidt, M. Gupta, J. Stahn, T. Gutberlet and M. Bruns, *Acta Mater.*, 2008, **56**, 464.

This journal is © the Owner Societies 2012

Phys. Chem. Chem. Phys., 2012, **14**, 2427–2433 | 2433